

The tricritical point of finite-temperature phase transitions in large N (Higgs) gauge theories.

Peter Arnold and David Wright

Department of Physics, University of Washington, Seattle, Washington 98195

(October 1996)

Abstract

Gauge theories broken by a single Higgs field are known to have first-order phase transitions in temperature if $\lambda/g^2 \ll 1$, where g is the gauge coupling and λ the Higgs self-coupling. If the theory is extended from one to N Higgs doublets, with $U(N)$ flavor symmetry, the transition is known to be second order for $\lambda/g^2 \gtrsim 1$ in the $N \rightarrow \infty$ limit. We show that one can in principle compute the tricritical value of λ/g^2 , separating first from second-order transitions, to any order in $1/N$. In particular, scalar fluctuations at the transition damp away the usual problems with the infrared behavior of high-temperature non-Abelian gauge theories. We explicitly compute the tricritical value of λ/g^2 for $U(1)$ and $SU(2)$ gauge theory to next-to-leading order in $1/N$.

This report was prepared as an account of work sponsored by the United States Government. Neither the United States nor the United States Department of Energy, nor any of their employees, nor any of their contractors, subcontractors, or their employees, makes any warranty, express or implied, or assumes any legal liability or responsibility for the product or process disclosed, or represents that its use would not infringe privately-owned rights. By acceptance of this article, the publisher and/or recipient acknowledges the U.S. Government's right to retain a non-exclusive, royalty-free license in and to any copyright covering this paper.

I. INTRODUCTION

The possibility of explaining the observed baryon number of the universe by physics occurring at the electroweak phase transition has, in recent years, renewed interest in understanding how to assess the existence, order, and strength of phase transitions in gauge theories, such as electroweak theory, where gauge bosons get mass by the Higgs mechanism. The phase structure of the electroweak sector of the minimal standard model, with a single Higgs doublet, makes a good starting point for exploring such transitions. It has long been appreciated [1] that the phase transition is first-order in the limit that the zero-temperature Higgs boson mass is small compared to the W boson mass, *i.e.* when $\lambda \ll g^2$, where g is the electroweak gauge coupling and λ is the Higgs self-coupling. In this limit, a perturbative analysis of the phase transition is adequate to establish its order and compute its physical properties. (Here and throughout, we assume λ and g^2 are both small.) What has been more difficult is to study the transition when $\lambda \gtrsim g^2$. In this limit, perturbation theory breaks down due to large infrared fluctuations characteristic of critical or near-critical behavior. One response is to turn to numerical simulations of the transition. It is interesting, however, to see what can be said about the transition analytically if one modifies the theory to make it more tractable. For example, if the three spatial dimensions are replaced by $4-\epsilon$ dimensions, where $\epsilon \ll 1$, then it is known that the transition remains first-order for any finite λ/g^2 [2,3]. If the Higgs sector is generalized to contain N Higgs doublets with $U(N)$ symmetry, then in the $N \rightarrow \infty$ limit the transition is first-order for $\lambda/g^2 \ll 1/N$ and second-order for $\lambda/g^2 \gg 1/N$ [3]. Recent numerical simulations for $N=1$, in contrast, suggest that the first-order transitions end at a critical value of λ/g^2 above which there is no phase transition whatsoever [4].¹

¹ We should emphasize that one of the pieces of evidence presented in ref. [4]—the large volume dependence of the $\Phi^\dagger\Phi$ susceptibility—has a loophole which is realized in a simple and relevant example. Ref. [4] shows evidence that this susceptibility approaches a constant in the large volume limit, for Higgs masses above roughly 80 GeV. In a second-order transition, the large volume behavior of this susceptibility should be

The goal of the present work is to extend understanding of the large N limit beyond leading order in $1/N$, studying in particular the critical value of λ/g^2 demarking the end of first-order transitions. We emphasize that large N here refers to the number of scalar fields and not to the replacement of the gauge group by $SU(N)$.

Usually, studying critical behavior of weakly coupled field theories is *more* difficult than studying those theories far from the transition, because long-distance fluctuations appear at the transition whose physics is non-perturbative. Small N pure scalar theories, for example, are easy to study far from the transition but difficult near the transition for this reason. Amusingly, large N (scalar) non-Abelian gauge theories are exactly the opposite: At temperatures far above the transition, electric forces are Debye screened in the hot plasma but magnetic forces are not, and the non-Abelian nature of the forces gives rise to magnetic confinement at large distances, which cannot be treated perturbatively. But, as we shall discuss, *at* the phase transition long-distance scalar fluctuations screen the magnetic forces sufficiently to prevent magnetic confinement. The long-distance scalar fluctuations themselves are treatable in a $1/N$ expansion just as in large N pure scalar theories.

In the remainder of this introduction, we briefly discuss how large one might suspect N has to be for the large N expansion to be useful. Then we discuss whether a moderately large N Higgs sector is phenomenologically viable. In section 2, we will fix notation and briefly review that the problem of finite temperature phase transitions in 3+1 dimensions is equivalent to the study of field theories in 3 Euclidean dimensions. Then we discuss the power counting of the loop expansion and why magnetic confinement is not a problem at

an analytic function of V^{-1} plus a non-analytic scaling piece whose leading term is $V^{\alpha/3\nu}$, where α and ν are respectively the specific heat and correlation length exponents. However, there are systems with second-order transitions where α/ν is *negative*, and so the measured susceptibility would indeed approach a constant rather than diverge. A relevant example is the pure scalar sector of electroweak theory itself, the $O(4)$ model, where $\alpha/3\nu = -0.33(4)$ (see table I). A more convincing demonstration of the absence of a transition is the plot in ref. [4] of the inverse correlation length vs. temperature, which shows no suggestion of a divergence in the correlation length.

the transition. We will also see that the calculation of the tricritical value of λ/g^2 order by order in $1/N$ is conceptually more straightforward than the calculation of many other quantities. In section 3, we carry out this computation to next-to-leading order for the U(1) gauge theory. Section 4 is devoted to clearing up some minor subtleties of regularization of diagrams. Finally, we carry out the next-to-leading order computation for SU(2) theory in section 5. same for SU(2) theory in section 5.

A. How large in large N ?

If gauge interactions are ignored, the scalar sector of the minimal standard model with a *single* Higgs doublet is equivalent to an O(4) theory of four real scalar fields and has a second-order transition. Table I demonstrates large N results applied to this case ($g=0$). Amusingly, next-to-leading order in $1/N$ actually gets in the right ballpark for various critical exponents. Sadly, this happy circumstance that 1 is just on the verge of being a large number of doublets will not survive the inclusion of gauge interactions.

	Large N			actual	
	LO	NLO	NNLO	series	monte carlo
$\gamma =$	2	1.392	1.188	1.44(4)	1.477(18)
$\nu =$	1	0.730	0.612	0.73(2)	0.7479(90)
$\beta =$	0.5	0.399	0.325	0.38(1)	0.3836(46)
$\delta =$	5	4.594	4.695	4.82(5)	4.851(22)
$\eta =$	0.0675	0.0554	0.0260	0.03(1)	0.0254(38)
$\alpha =$	-1	-0.189	0.163	-0.19(6)	-0.244(27)

TABLE I. Large N expansion results [5] for critical exponents in the pure scalar case ($g=0$) for one Higgs doublet: the O(4) model. Results are given for leading (LO), next to leading (NLO), and next to next to leading (NNLO) order in $1/N$. The actual values, as predicted from series analysis ([6] as cited in [7]) or measured by monte carlo [8], are also shown. There are various scaling relationships between these quantities, so that only two of the above exponents are independent.

At another extreme, one can analyze the phase structure for arbitrary N in $4 - \epsilon$ spatial dimensions [9,3]. One finds that the qualitative picture given by the large N limit—that there is a tricritical value of λ/g^2 above which the transition is second order—is correct when

$$N > 182.95 - 320.50\epsilon + O(\epsilon^2), \quad \text{for U(1) with } N \text{ charged scalars,} \quad (1.1)$$

$$N > 359 - 495.4\epsilon + O(\epsilon^2), \quad \text{for SU(2) with } N \text{ scalar doublets.} \quad (1.2)$$

So, near four spatial dimensions, large N means $N \gg 183$ or $N \gg 359$, respectively!

A result of our calculation of the tricritical point will be that quantitative success of large N in three dimensions appears to require $N \gg 4$ charged scalars for U(1) theory and $N \gg 20$ doublets for SU(2) theory.

B. Is moderately large N phenomenologically viable?

Generalizing the one Higgs model to a $U(N)$ Higgs model is motivated solely by the desire to find a theory whose phase transition is analytically tractable. Nonetheless, it's interesting to briefly consider (just for fun!) whether such a model might be consistent with real world phenomenology.

A $U(N)$ flavor-symmetric Higgs sector is a phenomenological disaster because electroweak symmetry breaking will break the global $U(N)$ and produce massless Goldstone bosons. The essential difference between Higgs models susceptible to large N (scalar) analysis and generic multiple Higgs models is the necessity of a large N global symmetry. There is no reason, however, that this symmetry need be continuous. Though we do not study it in this paper, one could instead have a Higgs sector with a *discrete* N -flavor permutation symmetry:²

² The purely scalar sector is a simple generalization of the cubic anisotropy model. See, for example, ref. [10].

$$\begin{aligned} \mathcal{L} \sim & |D\vec{\Phi}|^2 + m^2|\vec{\Phi}|^2 + \lambda_1|\vec{\Phi}|^4 + \lambda_2 \sum_i (\Phi_i^* \Phi_i)^2 \\ & + g_u \bar{Q}_R (\Phi_1 + \cdots + \Phi_N) u_L + g_d \bar{Q}_R \tau_2 (\Phi_1 + \cdots + \Phi_N)^* d_L. \end{aligned} \quad (1.3)$$

As an added bonus, the permutation symmetry prevents the tree-level flavor-changing neutral currents that plague generic multiple scalar models.

Because the discrete flavor symmetry is spontaneously broken, the model suggested above will produce cosmological domain walls which overclose the universe. This problem could be solved by the introduction of a very small symmetry breaking term (which is natural in the sense of 't Hooft [11]) that would cause the domain walls to coalesce after they were formed.

Some sort of $N > 1$ models therefore seem acceptable phenomenologically. It is worth noting that there is an important qualitative difference between the $N = 1$ and $N > 1$ cases. For $N > 1$ there is, by construction, a *global* flavor symmetry that is spontaneously broken at the electroweak scale. Such models therefore always have some sort of phase transition (ignoring the tiny symmetry breaking term discussed above). The $N = 1$ model, in contrast, need not have a transition because, technically, local symmetries are never spontaneously broken due to Elitzur's theorem [12,4].

We shall not analyze in any detail just how large N could be in a realistic theory except to make one, trivial observation: there is a simple constraint from triviality. Non-perturbative continuum scalar theories are not well defined, and the effective strength of scalar interactions is $O(N\lambda)$ instead of $O(\lambda)$. The largest Higgs mass for which the theory can be sensible as an effective theory therefore decreases roughly as $1/\sqrt{N}$ from the $N=1$ limit of $O(1 \text{ TeV})$. $N \gg 100$ is clearly out of the picture. On a related note, $N > 20$ would destroy the asymptotic freedom of the $SU(2)$ electroweak interactions in the standard model.

One can imagine that N might be big enough for the large N approximation to be reasonable, but not too big to run into phenomenological problems. There's no good reason, of course, why nature would choose to be so peculiar.

II. LARGE N COUNTING

The problem of studying a second-order (or very weakly first-order) phase transition in weakly coupled quantum field theory, as one varies the temperature, can be reduced to the problem of studying the phase transition in three-dimensional Euclidean field theory, as one varies a mass. In our case, the three-dimensional theory is of the form

$$S = \int d^3x \left\{ |D\vec{\Phi}|^2 + \frac{1}{4}F^2 + m^2|\vec{\Phi}|^2 + \frac{1}{6}\lambda|\vec{\Phi}|^4 + \frac{1}{90}\eta|\vec{\Phi}|^6 \right\}, \quad (2.1)$$

and the transition occurs as m^2 is varied through zero. Let's take a moment to briefly review this correspondence.

Critical or near-critical behavior of phase transitions is governed by the physics of long distances, which in our case is classical. It is classical because the Bose density per mode, $1/(e^{-\beta E} - 1)$, becomes large for small energies E . So one may study the long-distance, equilibrium properties of such transitions by studying the classical statistical mechanics of field theory in three spatial dimensions. More formally, one may start with the Euclidean formulation of finite-temperature quantum field theory and then integrate out the physics of the small, periodic Euclidean time direction. (See refs. [13] for a review.) Taking the additional step of integrating out the Debye-screened A_0 field, one obtains an effective three-dimensional theory of the form (2.1) plus irrelevant interactions. The parameters of the effective three-dimensional theory can be perturbatively related to those of the original 3+1 dimensional theory if the couplings are small. One finds, up to higher-order corrections, that

$$g^2 = g_4^2(T) T, \quad \lambda = \lambda_4(T) T, \quad \eta = O(g_4^6, \lambda^3), \quad (2.2)$$

where $g_4(T)$ and $\lambda_4(T)$ are the dimensionless couplings of the 3+1 dimensional theory at a renormalization scale of order the temperature T . One also finds that increasing the temperature through the transition corresponds to varying the scalar mass m in the effective theory from $m^2 < 0$ to $m^2 > 0$. So the problem of understanding the phase transition of the

original theory in temperature is equivalent to understanding the phase transition of a three-dimensional theory in m^2 . In the limit that the original couplings g_4^2 and λ_4 are considered arbitrarily small, the problem of finding the tricritical value of λ_4/g_4^2 in the original theory is the same as finding the tricritical value of λ/g^2 in the three-dimensional theory.

So focus on the three-dimensional theory (2.1), and note that λ and g^2 have dimensions of mass. Now consider the naive perturbative expansion for some physical observable associated with a small momentum scale p and suppose we are in the symmetric phase $m^2 > 0$ and that $p \ll m$. Then the scalars will decouple, and we must focus on the non-Abelian interactions of the magnetic gauge fields. (As mentioned earlier, the electric ones are Debye screened.) By dimensional analysis, the loop expansion parameter for gauge interactions is then g^2/p , and perturbation theory will fail once we try to explore momentum scales $p \lesssim g^2$. This is the source of the infrared problem for non-Abelian gauge theories at high temperature.

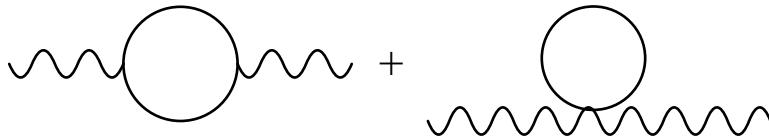


FIG. 1. Leading contribution to the gauge boson self-energy.

Now consider the case right at a second-order transition, where the scalar mass is zero, and consider the effect of the self-energy diagrams of fig. 1 on the gauge boson propagator. By dimensional analysis, this self-energy is

$$\Pi(p) = aNg^2p, \quad (2.3)$$

where a is a numerical constant, and the gauge propagator becomes

$$G(p) \sim \frac{1}{p^2 + aNg^2p} \rightarrow \frac{1}{aN g^2 p} \quad \text{as } p \rightarrow 0. \quad (2.4)$$

This is less divergent in the infrared than the perturbative propagator $1/p^2$. For distances $r \gg 1/Ng^2$, the scalar degrees of freedom have screened the gauge propagator from $1/r$

behavior to $1/r^2$ behavior. The problematical interactions above the phase transition were non-Abelian gauge interactions. Now, with the propagator (2.4), such interactions are under perturbative control for large N . Loops of gauge bosons will in general be infrared convergent, and the scale of the loop momenta will be $O(Ng^2)$ if the external momentum is small. The cost of adding a new pair of non-Abelian interactions to a graph, such as depicted in fig. 2, is then, by dimensional analysis, generically

$$g^2 \times \frac{1}{Ng^2} \sim \frac{1}{N}. \quad (2.5)$$

The double lines represent the resummed gauge propagator (2.4).

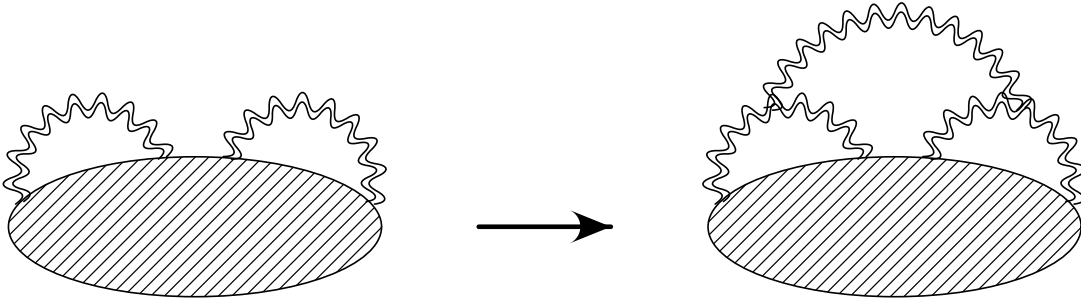


FIG. 2. Adding a pair of non-Abelian interactions to a graph.

We have now discussed the cost of adding purely gauge loops to a diagram. Before proceeding to the case of generic scalar loops in a diagram, it will be useful to first review the leading-order calculation of ref. [3] for the tricritical value of λ/g^2 .

A. Tricritical point at leading order

For a second-order phase transition, the transition occurs when the effective mass of the scalar field vanishes. A tricritical point occurs when the effective, low-momentum, quartic coupling λ_{eff} of the scalar vanishes as well. The classic mean-field example is the potential

$$V = \frac{1}{2}m^2|\vec{\Phi}|^2 + \frac{1}{4!}\lambda|\vec{\Phi}|^4 + \frac{1}{6!}\eta|\vec{\Phi}|^6, \quad (2.6)$$

which (ignoring corrections due to fluctuations) has a second-order transition in m^2 if $\lambda > 0$, a first-order transition in m^2 if $\lambda < 0$, and a tricritical point at $\lambda = 0$. The actual low-momentum effective potential for gauge-Higgs theories was computed at leading order in $1/N$ in ref. [3]. Here, we just need the effective value of the four-point interaction. We begin by assuming λ/g^2 is $O(N^{-1})$, which we shall see *a posteriori* is the correct place to look for the tricritical point. For simplicity, we will also ignore the bare six-point coupling η by setting it to zero.³ The theory is then super-renormalizable. λ and g^2 do not require renormalization and will henceforth refer to their bare, short-distance values.

It is convenient to henceforth think of g^2 as $O(N^{-1})$ and so λ as $O(N^{-2})$. This is just a convention because g^2 is dimensionful, but it is a convenient convention because it makes the internal momenta of gauge bosons in the graphs discussed above $O(N^0)$. N counting of those graphs then reduces to counting scalar loops and explicit coupling constants.

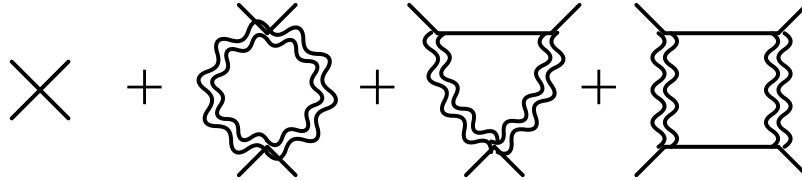


FIG. 3. Leading-order contributions to the scalar four-point interaction.

The leading-order graphs for the four-point interaction are shown in fig. 3, where the double lines again represent the resummed gauge propagator (2.4). For the U(1) case, these graphs give

$$\lambda_{\text{eff}} = \lambda - 12g^4 \int \frac{d^3p}{(2\pi)^3} \frac{1}{(p^2 + aNg^2p)^2} = \lambda - \frac{6g^2}{\pi^2 aN}, \quad (2.7)$$

where computation of the self-energy diagrams fig. 1 yields

³ This is sensible, based on (2.2), if one formally considers g_4^2 to be arbitrarily small. If one instead considers the natural choice that g_4^2 is $O(N^{-1})$, then η will be $O(N^{-3})$. At the order under consideration, the effects of η on the following derivation can be absorbed into the definition of λ .

$$\Pi_{\mu\nu}(p) = aNg^2p \left(\delta_{\mu\nu} - \frac{p_\mu p_\nu}{p^2} \right), \quad a = \frac{1}{16}. \quad (2.8)$$

Setting λ_{eff} to zero, the tricritical point is at

$$\frac{\lambda}{g^2} = \frac{96}{\pi^2 N} + O(N^{-2}). \quad (2.9)$$

The case of $\text{SU}(2)$ with N doublet Higgs bosons differs just by the number of gauge bosons and the normalization of the coupling of the scalars to the gauge bosons. With conventional normalization of g ,

$$\frac{\lambda}{g^2} = \frac{36}{\pi^2 N} + O(N^{-2}). \quad (2.10)$$

B. Scalar loops in the infrared

Consider for a moment pure scalar theory. At zero external momentum, the naive loop expansion parameter is $N\lambda/m$, where the $1/m$ follows from dimensional analysis. There is therefore an infrared problem when one goes to the transition, $m \rightarrow 0$. The standard application of large N techniques to this theory eradicates this problem by a large N resummation of the quartic interaction, which curbs the infrared behavior of the diagrammatic expansion.⁴

In gauge-Higgs theories, the same problem potentially arises and will require a similar resummation of the scalar interactions. However, for the special case of computing the tricritical value of λ/g^2 , this resummation is unnecessary. Because the problem with the naive expansion in scalar loops was an infrared problem, the loop expansion parameter $N\lambda/m$ due to the infrared behavior ($p \ll Ng^2$) of loops should be replaced by $N\lambda_{\text{eff}}/m$. But λ_{eff} at the tricritical point is zero by definition. As we have reviewed, that zero occurs because of a cancelation of interactions, such as those shown at leading order in fig. 3. This

⁴ This is most easily achieved by the standard technique of replacing the quartic interaction $\lambda\phi^4$ by $\chi^2 + \sqrt{\lambda}\phi^2\chi$ where χ is an auxiliary field, integrating out ϕ , and then studying the resulting theory of χ .

cancellation breaks down for loop momenta $p \gtrsim Ng^2$, so the real cost of adding a scalar loop at the tricritical point will be determined by the scale Ng^2 :

$$\frac{N\lambda}{p} \sim \frac{\lambda}{g^2} \sim \frac{1}{N}. \quad (2.11)$$

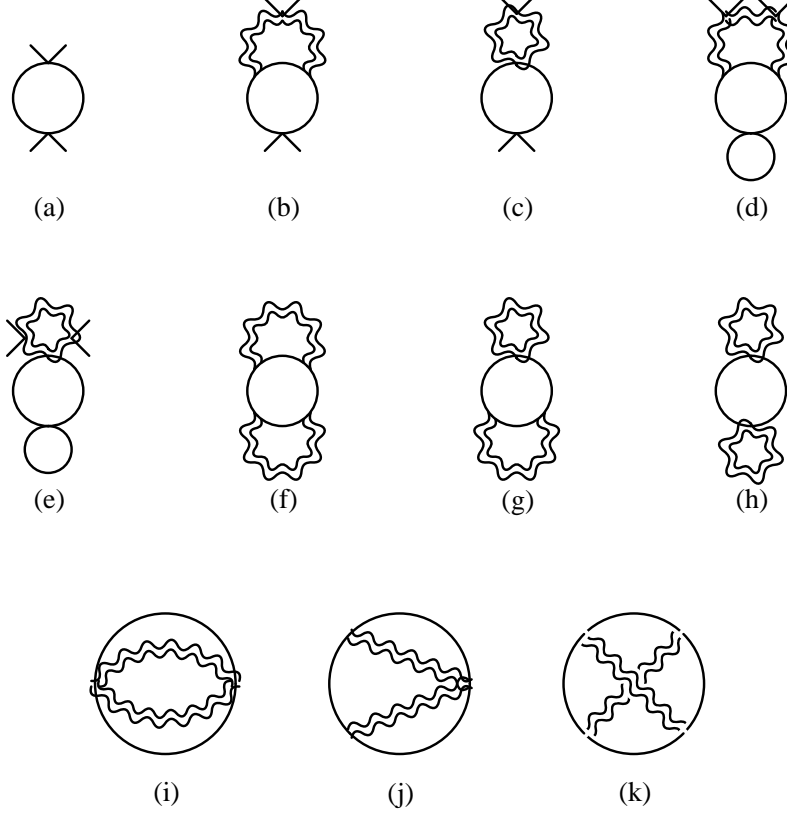


FIG. 4. Next-to-leading order contributions to the scalar four-point interaction: abelian graphs. We have neglected graphs that vanish in the Abelian case due to Furry's theorem, *i.e.* charge conjugation. See fig. 7 for interpretation of (f–k).

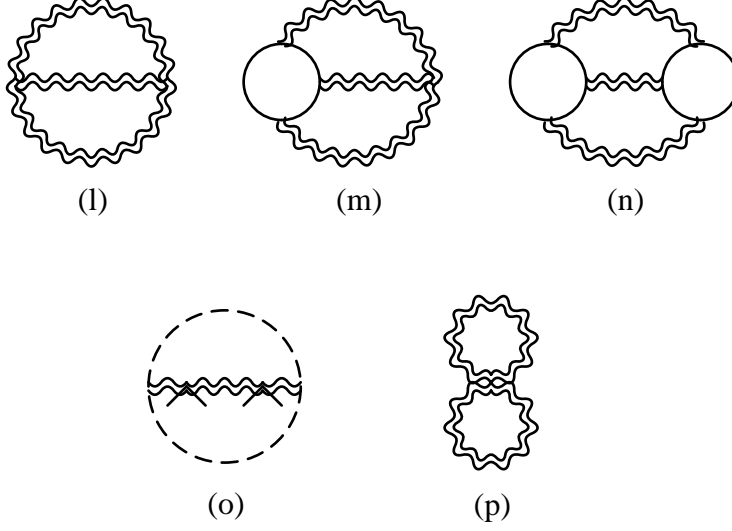


FIG. 5. Next-to-leading order contributions to the scalar four-point interaction: $SU(2)$ graphs in Landau gauge. We have neglected graphs which vanish by charge conjugation. Note that the subgraph of fig. 6 vanishes for $SU(2)$ but not other groups. The dashed lines represent ghosts. See fig. 7 for interpretation of (l-n,p).

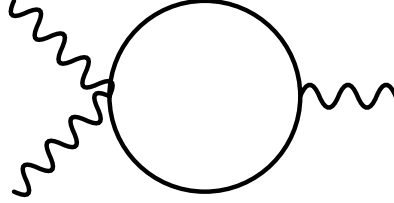


FIG. 6. A subgraph which vanishes for $U(1)$ and $SU(2)$.

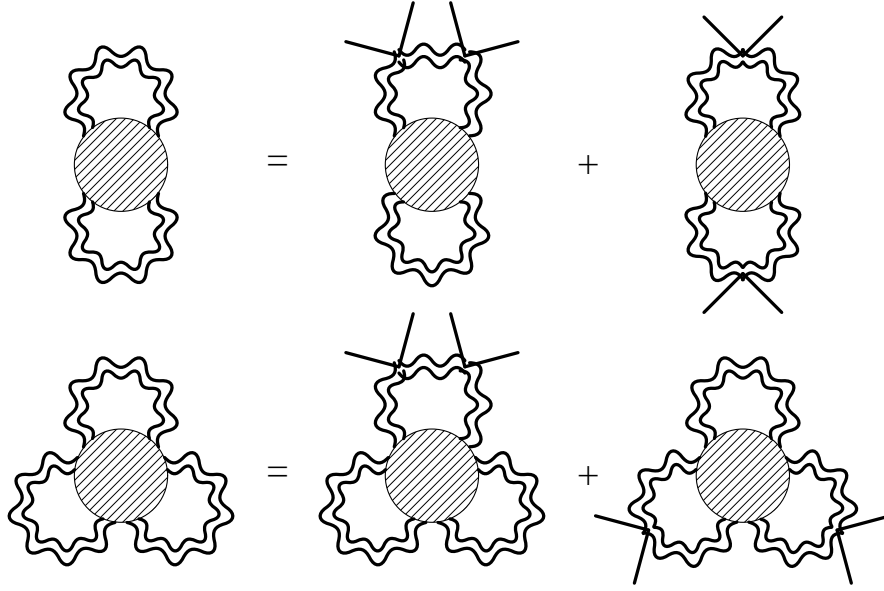


FIG. 7. Meaning of abbreviated graphs in figs. 4 and 5.

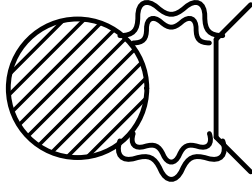


FIG. 8. Example of diagrams which vanish in Landau gauge for zero external momentum.

The upshot is that, to determine the tricritical point, we can set $m=0$ and then use naive large N power-counting of diagrams, treating $g^2 \sim O(N^{-1})$ and $\lambda \sim O(N^{-2})$. The relevant diagrams for computing λ_{eff} at next-to-leading order in $1/N$ are shown in figs. 4 and 5 for Landau gauge. In this gauge, diagrams of the form of fig. 8 vanish at zero external momentum. The graphs (f-n,p) denote the contributions to λ_{eff} in the short-hand style explained by fig. 7. At each order in the calculation of λ_{eff} , and the simultaneous determination of the tricritical point by setting $\lambda_{\text{eff}} = 0$, one will find that scalar infrared divergences always cancel at the order one is calculating. We now turn to a calculation of the U(1) case, corresponding to the diagrams fig. 4, where this will be made explicit.

III. U(1) TRICRITICAL POINT: NEXT-TO-LEADING ORDER

For simplicity, we shall present the calculation in Feynman gauge. The total contribution of diagrams of the form of fig. 8 still vanishes in the U(1) case because of the U(1) Ward identity of fig. 9.⁵ (Landau gauge results, which will be useful for the SU(2) case, are given in Appendix B 2.)

$$p_\mu \quad \text{[diagram]} \quad = 0$$

FIG. 9. A U(1) Ward identity.

We shall proceed by doing the scalar loop integrals of all the diagrams of fig. 4, summing up the diagrams, and then integrating over the gauge boson momenta. The order of the last two steps is important because the gauge momentum integrals are infrared divergent for the individual diagrams but not for the sum, and it will be convenient not to have to introduce a consistent infrared regulator. (Our disregard of regularization will sometimes be a bit cavalier in this section, and we delay discussion of potential subtleties to section 4.)

As a warmup, consider fig. 4i. This diagram gives a contribution to λ_{eff} of

$$\delta\lambda_{\text{eff}}^{(i)} = -72Ng^8 \int_{pq} \mathcal{F}_{pq} \int_l \frac{1}{l^2(1+\mathbf{p}+\mathbf{q})^2} = -Ng^8 \int_{pq} \mathcal{F}_{pq} \frac{9}{|\mathbf{p}+\mathbf{q}|}, \quad (3.1)$$

where we have introduced the notation

$$\int_p \equiv \int \frac{d^3p}{(2\pi)^3}, \quad (3.2)$$

$$\mathcal{F}_{pq} \equiv f_p^3 f_q + f_p^2 f_q^2 + f_p f_q^3, \quad (3.3)$$

and f_p is the large N resummed gauge propagator

⁵ We have checked this explicitly. We have also explicitly checked our final U(1) results are the same in any covariant gauge.

$$f_p \equiv \frac{1}{p^2 + aNg^2p}. \quad (3.4)$$

A useful table of various l integrals is given in Appendix A.

As a slightly more complicated example, consider fig. 4j, which gives

$$\delta\lambda_{\text{eff}}^{(j)} = 48Ng^8 \int_{pq} \mathcal{F}_{pq} \int_l \frac{(2\mathbf{l} - \mathbf{p}) \cdot (2\mathbf{l} + \mathbf{q})}{l^2(\mathbf{l} - \mathbf{p})^2(\mathbf{l} + \mathbf{q})^2}. \quad (3.5)$$

To simplify the l integration, one may use the standard technique of rewriting numerators in terms of denominators and things that don't involve l :

$$(2\mathbf{l} - \mathbf{p}) \cdot (2\mathbf{l} + \mathbf{q}) = (\mathbf{l} - \mathbf{p})^2 + (\mathbf{l} + \mathbf{q})^2 + 2l^2 - (p^2 + \mathbf{p} \cdot \mathbf{q} + q^2), \quad (3.6)$$

giving

$$\begin{aligned} \delta\lambda_{\text{eff}}^{(j)} &= 48Ng^8 \int_{pq} \mathcal{F}_{pq} \int_l \left[\frac{1}{l^2(\mathbf{l} + \mathbf{q})^2} + \frac{1}{l^2(\mathbf{l} - \mathbf{p})^2} + \frac{2}{(\mathbf{l} - \mathbf{p})^2(\mathbf{l} + \mathbf{q})^2} - \frac{(p^2 + \mathbf{p} \cdot \mathbf{q} + q^2)}{l^2(\mathbf{l} - \mathbf{p})^2(\mathbf{l} + \mathbf{q})^2} \right] \\ &= Ng^8 \int_{pq} \mathcal{F}_{pq} \left[\frac{6}{q} + \frac{6}{p} + \frac{12}{|\mathbf{p} + \mathbf{q}|} - \frac{6(p^2 + \mathbf{p} \cdot \mathbf{q} + q^2)}{pq|\mathbf{p} + \mathbf{q}|} \right] \end{aligned} \quad (3.7)$$

Appendix A explains an amusingly simple method for evaluating the last l integral by using a simple change of variables.

Fig. 4k can be done similarly, and the result is given in Appendix B.

Figs. 4(a–h) are slightly more subtle because the scalar integration is infrared divergent, both diagram by diagram and collectively. For instance fig. 4a gives

$$\delta\lambda_{\text{eff}}^{(a)} = -\frac{\lambda^2}{3} \int_l \frac{1}{l^4}. \quad (3.8)$$

However, as we discussed earlier, λ should end up replaced by $\lambda_{\text{eff}} = 0$ in the infrared if we sum up diagrams, as was shown at leading-order in fig. 3. The cancelation in fig. 3 will correspond to a cancelation, at this order in $1/N$, in the diagrams of fig. 4(a–c,f–h) if we consider the pieces of (f–h) represented by the *second* term on the right-hand side of fig. 7a.⁶ That is, if we set

⁶ Keep in mind that the last two terms of fig. 3 can be ignored on the context of the NLO diagrams (a–h) because of the Ward identity of fig. 9.

$$\lambda = \frac{96}{\pi^2 N} g^2 + O(N^{-2}) \quad (3.9)$$

to make λ_{eff} zero at leading order, then we will find that the infrared divergences just discussed will cancel each other at the order in $1/N$ at which we are computing. It will be convenient to write this condition at a more primitive level, related directly to the diagrams of fig. 3, as

$$\lambda = 12C_\lambda g^4 \int_p f_p^2, \quad (3.10)$$

where the value of λ is now parametrized by C_λ and

$$C_\lambda = 1 + O(N^{-1}) \quad (3.11)$$

at the tricritical point.

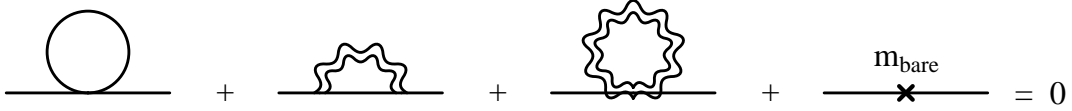


FIG. 10. Diagrams contributing to the effective scalar mass m_{eff} .

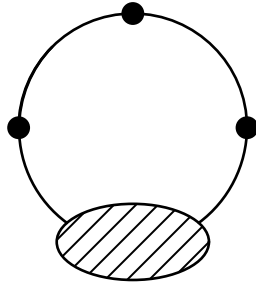


FIG. 11. IR divergent loops caused by treating a non-zero mass perturbatively. The circles represent mass insertions on a massless propagator.

There still remain infrared divergences, however, in the pieces of figs. 4(d–h) corresponding to the *first* term on the right-hand side of fig. 7a. The divergence does not cancel in the sum of these graphs because, though we have taken $m = 0$ in our perturbative scalar propagators, we have so far ignored the fact that radiative corrections such as the first three

diagrams of fig. 10 will generate a contribution to the mass. And if the mass of a massive scalar is treated perturbatively, it will generate infrared divergences, such as depicted by fig. 11, which shows massless propagators connecting a perturbative mass insertion. To be at the transition $m_{\text{eff}} = 0$, we need to fine-tune the bare mass at this order to satisfy the equation of fig. 10. An application of the Feynman rules for these diagrams shows that this requires

$$m_{\text{bare}} = -2g^2 \int_p f_p - \frac{2}{3}N\lambda \int_p \frac{1}{p^2} + (\text{higher order}). \quad (3.12)$$

If we treat m_{bare} perturbatively, it will cancel the radiative contributions to the mass order by order in perturbation theory. All we need to do to cancel the infrared divergences in our calculation of λ_{eff} at this order is to include the additional diagrams of fig. 12. We will henceforth ignore the graphs of figs. 4d and e and the second term of the bare mass (3.12) above, as these trivially cancel each other.

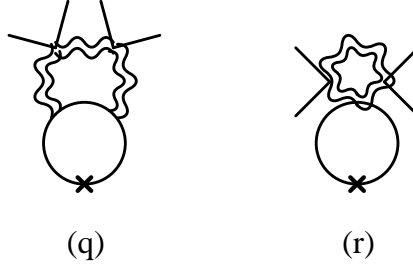


FIG. 12. Additional NLO diagrams, containing bare mass insertion.

The graph of fig. 4f gives a contribution to $\delta\lambda_{\text{eff}}$ of

$$-12Ng^8 \int_{pq} \mathcal{F}_{pq} \int_l \frac{(2\mathbf{l} - \mathbf{p})^2 (2\mathbf{l} + \mathbf{q})^2}{l^4 (1 - \mathbf{p})^2 (1 + \mathbf{q})^2}; \quad (3.13a)$$

the graphs of figs. 4(b,g) and 12q give

$$-12Ng^8 \int_{pq} [f_p f_q^3 + (3 - 2C_\lambda) f_p^2 f_q^2 + 3f_p^3 f_q] \int_l \left[-\frac{(2\mathbf{l} + \mathbf{q})^2}{l^4 (1 + \mathbf{q})^2} \right] - 12Ng^8 \{p \leftrightarrow q\}; \quad (3.13b)$$

and the graphs of figs. 4(a,c,h) and 12r give

$$-12Ng^8 \int_{pq} [3f_p f_q^3 + (3 - 2C_\lambda)^2 f_p^2 f_q^2 + 3f_p^3 f_q] \int_l \frac{1}{l^4}. \quad (3.13c)$$

Now consider the sum of (3.13a–c). Setting C_λ to 1, we find that the l integral of the sum of the integrands converges, as promised.⁷

Having verified that the infrared divergences cancel, it is convenient to proceed by computing the various terms individually, regulating the l integration with dimensional regularization. The results are given in Appendix B.

The next step is to do the p and q integrations. We do this by first performing the integration over the relative angle θ between \mathbf{p} and \mathbf{q} . As an example, consider fig. 4j again and our result (3.7). By using the angular averages

$$\left\langle \frac{1}{|\mathbf{p} + \mathbf{q}|} \right\rangle_\theta = \frac{1}{p_>} \quad \text{and} \quad \left\langle \frac{\cos \theta}{|\mathbf{p} + \mathbf{q}|} \right\rangle_\theta = -\frac{p_<}{3p_>^2}, \quad (3.14)$$

we obtain

$$\delta\lambda_{\text{eff}}^{(j)} = Ng^8 \int_{pq} \mathcal{F}_{pq} \frac{1}{p_>} (18 - 4x), \quad (3.15)$$

where

$$p_> \equiv \max(p, q), \quad p_< \equiv \min(p, q), \quad x \equiv p_</p_>. \quad (3.16)$$

Similar results for the rest of the graphs are given in Appendix B. The sum of all graphs gives

$$\delta\lambda_{\text{eff}} = Ng^8 \int_{pq} \mathcal{F}_{pq} \frac{h(x)}{p_>} + Ng^8 \int_{pq} f_p^3 f_q \left[\frac{12}{q} \right], \quad (3.17)$$

$$h(x) = -6 + \frac{11}{2}x + 3x^{-1} - \left(\frac{15}{2} + 3x^{-2} + 3x^2 \right) (1 + x^2)^{-1/2} \text{Sinh}^{-1}x. \quad (3.18)$$

To do one of the integrals easily, write

$$\begin{aligned} \int_{pq} \mathcal{F}_{pq} \frac{h(x)}{p_>} &= \frac{1}{2\pi^4} \int_0^\infty p^2 dp \int_0^p q^2 dq \mathcal{F}_{pq} \frac{h(q/p)}{p} \\ &= \frac{1}{2\pi^4} \int_0^1 dx x^2 h(x) \int_0^\infty dp p^4 (f_p f_{xp}^3 + f_p^2 f_{xp}^2 + f_p^3 f_{xp}) \\ &= \frac{-1}{2\pi^4 a^3 N^3 g^6} \int_0^1 \frac{dx}{x} \left[\frac{(1+x)}{(1-x)} \ln x + \frac{3}{2} \right] (1+x) h(x), \end{aligned} \quad (3.19)$$

⁷ More accurately, it converges if one ignores logarithmic infrared divergences $\int_l (1/l^4)$ that vanish by parity. The physical regulator—an arbitrarily tiny mass term due to being infinitesimally above the transition—respects parity. Dimensional regularization does also.

and similarly

$$\int_{pq} f_p^3 f_q \frac{1}{q} = \frac{-1}{4\pi^4 a^3 N^3 g^6} \int_0^1 \frac{dx}{x(1-x)^2} \left[\frac{(1+x^3)}{(1-x)} \ln x + \frac{3}{2} - x + \frac{3}{2} x^2 \right]. \quad (3.20)$$

Combining them gives

$$\delta\lambda_{\text{eff}} = -\frac{\kappa g^2}{2\pi^4 a^3 N^2} = -\frac{2048 \kappa g^2}{\pi^4 N^2}, \quad (3.21)$$

where

$$\begin{aligned} \kappa = \int_0^1 \frac{dx}{x} \left\{ \left[\frac{(1+x)}{(1-x)} \ln x + \frac{3}{2} \right] (1+x) h(x) \right. \\ \left. + \frac{6}{(1-x)^2} \left[\frac{(1+x^3)}{(1-x)} \ln x + \frac{3}{2} - x + \frac{3}{2} x^2 \right] \right\}. \end{aligned} \quad (3.22)$$

The contributions of each diagram to κ contain logarithmic divergences at small x , but the total is integrable. The integral can in principal be done analytically, with the result expressed in terms of generalized polylogarithms with arguments like $\sqrt{2}$, but this seems unhelpful enough that we haven't bothered.⁸ Numerical integration gives

$$\kappa = 1.68536... \quad (3.23)$$

The final results for the tricritical value of λ/g^2 is then

$$\begin{aligned} \lambda/g^2 &= \frac{96}{\pi^2} \left[N^{-1} + \frac{64\kappa}{3\pi^2} N^{-2} + O(N^{-3}) \right] \\ &= \frac{96}{\pi^2} \left[N^{-1} + 3.64293 N^{-2} + O(N^{-3}) \right]. \end{aligned} \quad (3.24)$$

IV. SOME REGULARIZATION ISSUES

In the last section, we did not bother to introduce a consistent regularization of divergences diagram by diagram, arguing that that divergences cancel when all diagrams were

⁸ The first step is to change variables to $y = x + \sqrt{1+x^2}$ in the terms involving $\text{Sinh}^{-1}x$, which then becomes $\ln y$. This transforms the integral into a product of rational functions and logarithms.

summed. This is a potentially dangerous argument and shall later plague us in the SU(2) calculation if we do not address it. To see the problem, consider the contributions of the form of fig. 13. The gauge loop integration would have an infrared divergence of the form

$$\int_p f_p^3 \Pi(0) \quad (4.1)$$

if the self-energy Π did not vanish at zero momentum. Fortunately, $\Pi(0) = 0$ is a consequence of Ward identities. The subtlety arises because $\Pi(0)$ does not necessarily vanish diagram by diagram. As an example, consider the *one*-loop contribution to $\Pi(0)$, as shown in fig. 1. Using dimensional regularization for the UV and a small scalar mass for the IR, these diagrams give

$$\Pi_{\mu\mu}(0) \approx -4g^2 \int_l \frac{l^2}{(l^2 + m^2)^2} + 2dg^2 \int_l \frac{1}{l^2}. \quad (4.2)$$

If we ignore the UV regularization and instead set $d = 3$ and combine the integrands, our l integral is *still* UV divergent. Our calculation (4.1) would then end up with ill-defined products of IR and UV divergences of the form

$$\int_{\text{IR}} \frac{d^3p}{p^3} \int_{\text{UV}} \frac{d^3l}{l^2}. \quad (4.3)$$

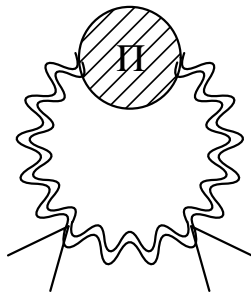


FIG. 13. A class of diagram with IR divergences in the gauge momentum.

The solution to avoiding this problem is to return to consistently regulating the theory. Then rewrite fig. 13 as

$$\int_p f_p^3 \Pi(0) = \int_p f_p^3 [\Pi(p) - \Pi(0)] + \int_p f_p^2 \Pi(0). \quad (4.4)$$

The p integration for the first term on the right is now IR convergent, and the calculation of $\Pi(p) - \Pi(0)$ is UV convergent diagram by diagram; so we can set $d = 3$ in this calculation and proceed as we did in the previous section. The second term on the right-hand side requires full regularization, but we know from Ward identities that $\Pi(0) = 0$, so we do not need to calculate it. The final prescription, then, is to replace $\Pi(p)$ by $\Pi(p) - \Pi(0)$ when computing diagrams like fig. 13.

The effect of this prescription on the U(1) calculation is that we should add by hand to (3.17) a term proportional to

$$\int_{pq} f_p^3 f_q \left[\frac{1}{q} \right] \quad (4.5)$$

in order to remove any remaining IR/UV divergences in the p/q integrals. However, no such term is needed, and so the prescription has no effect on our previous calculation.⁹ As we shall see, however, the prescription will be important to the SU(2) calculation of the next section.

V. SU(2) TRICRITICAL POINT: NEXT-TO-LEADING ORDER

The SU(2) case is more convenient to treat in Landau gauge than in Feynman gauge. This is because there are a host of diagrams, such as fig. 14, which vanish in Landau gauge for zero external momentum (because the gluon polarization the external scalars couple to is proportional to the gluon four-momentum and does not propagate in Landau gauge).

We will restrict our attention to the group SU(2) because it has the convenient property that scalar insertions such as shown in fig. 15 are proportional to $\delta_{ab}\delta_{ij}$. This greatly simplifies the analysis of the group factors in diagrams.¹⁰

⁹ This isn't an accident. The two loop contribution to $\Pi_{\mu\nu}(0)$ are UV log divergent diagram by diagram. For log divergences, cancelations are maintained even when the UV regularization is removed. Consider the example of (4.2) for $d=2$.

¹⁰ The quartic interaction $|\Phi|^4$ in (2.1) will mean $(\Phi_\alpha^\dagger \cdot \Phi^\alpha)^2$, where α is the SU(2) index. As noted in

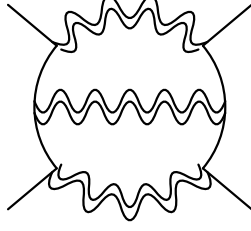


FIG. 14. A diagram which vanishes in Landau gauge.



FIG. 15. Scalar insertion on gauge line.

The Landau gauge results for the Abelian diagrams of fig. 4 are given in Appendix B 2. For $SU(2)$, they give the contribution

$$\delta\lambda_{\text{eff}}^{(a-k,q,r)} = Ng^8 \int_{pq} \mathcal{F}_{pq} \frac{h_1(x)}{p_{>}} + Ng^8 \int_{pq} f_p^3 f_q \left[\frac{27}{32q} \right], \quad (5.1)$$

$$h_1(x) = -\frac{27}{64} + \frac{15}{256}x - \frac{9}{160}x^2 - \frac{9}{128}x^{-1} + \left(\frac{45}{256} + \frac{9}{128}x^{-2} + \frac{9}{128}x^2 \right) (1+x^2)^{-1/2} \text{Sinh}^{-1}x. \quad (5.2)$$

In the $SU(2)$ case,

$$a = \frac{1}{32}, \quad (5.3)$$

and then

$$\delta\lambda_{\text{eff}}^{(a-k)} = -\frac{\kappa_1 g^2}{2\pi^4 a^3 N^2} = -\frac{2^{14} \kappa_1 g^2}{\pi^4 N^2}, \quad (5.4)$$

ref. [3], the theory with this interaction has a bigger global symmetry than simple flavor $U(N)$. The scalar sector has an $O(2N)$ symmetry. The gauge interactions reduce the symmetry to $SU(2)_L \times Sp(2N)_R$, where $Sp(2N)_R$ is the N -flavor generalization of the usual $SU(2)_R \simeq Sp(2)_R$ custodial symmetry of the $N=1$ case. This symmetry is larger than $U(N)$ and requires that the scalar potential be a function of only the single variable $\Phi_\alpha^\dagger \cdot \Phi^\alpha$, forbidding other possibilities such as $(\Phi_\alpha^\dagger \cdot \Phi^\beta)(\Phi_\beta^\dagger \cdot \Phi^\alpha)$. The appearance of such couplings severely complicates the generalization of our treatment to general gauge groups.

where

$$\begin{aligned}\kappa_1 &= \int_0^1 \frac{dx}{x} \left\{ \left[\frac{(1+x)}{(1-x)} \ln x + \frac{3}{2} \right] (1+x) h_1(x) \right. \\ &\quad \left. + \frac{27}{64(1-x)^2} \left[\frac{(1+x^3)}{(1-x)} \ln x + \frac{3}{2} - x + \frac{3}{2} x^2 \right] \right\} . \\ &= -0.052539(1)\end{aligned}\tag{5.5}$$

Now consider the non-Abelian graphs, and start with the ghost graph of fig. 5o. Doing the ghost loop integration, one finds

$$\delta\lambda_{\text{eff}}^{(o)} = f^{abc} f^{abc} g^2 \left[-\frac{3}{512\pi^2 a^2 N^2} - \frac{3}{8} \int_p f_p^3 \int_q \frac{1}{q^2} \right] \tag{5.6}$$

By our prescription for handling divergences, discussed in the previous section, the second term on the right-hand side should be discarded. For SU(2),

$$f^{abc} f^{abc} = 6. \tag{5.7}$$

The figure-eight graph of fig. 5p gives

$$\delta\lambda_{\text{eff}}^{(p)} = f^{abc} f^{abc} g^2 \left[\frac{1}{4\pi^4 a^2 N^2} + \int_{pq} f_q^3 f_p \left(\frac{9}{4} - \frac{3}{4} \cos^2 \theta \right) \right] \tag{5.8}$$

Again, the second term is thrown away by our prescription.

Finally, we have the graphs of fig. 5(l-n). Fig. 5(n), for example, is

$$\begin{aligned}\delta\lambda_{\text{eff}}^{(n)} &= -\frac{1}{32} f^{abc} f^{abc} g^6 \phi^4 \int_{pq} \mathcal{F}_{pqr} \\ &\quad \times \int_{l_1} \frac{(2l_1 - p)_\mu (2l_1 + q)_\nu (2l_1 - p + q)_\rho}{l_1^2 (\mathbf{l}_1 - \mathbf{p})^2 (\mathbf{l}_1 + \mathbf{q})^2} \int_{l_2} \frac{(2l_2 - p)_{\bar{\mu}} (2l_2 + q)_{\bar{\nu}} (2l_2 - p + q)_{\bar{\rho}}}{l_2^2 (\mathbf{l}_2 - \mathbf{p})^2 (\mathbf{l}_2 + \mathbf{q})^2} \\ &\quad \times \left(\delta_{\mu\bar{\mu}} - \frac{p_\mu p_{\bar{\mu}}}{p^2} \right) \left(\delta_{\nu\bar{\nu}} - \frac{q_\nu q_{\bar{\nu}}}{q^2} \right) \left(\delta_{\rho\bar{\rho}} - \frac{r_\rho r_{\bar{\rho}}}{r^2} \right),\end{aligned}\tag{5.9}$$

where

$$\mathbf{r} = \mathbf{p} + \mathbf{q} \tag{5.10}$$

and

$$\mathcal{F}_{pqr} = 3f_p^3 f_q f_r + 3f_p^2 f_q^2 f_r. \tag{5.11}$$

(If one prefers, one can symmetrize the definition of \mathcal{F}_{pqr} with respect to permutations.) We have evaluated the scalar integrals by brute force, and various Feynman and momentum integrals required for this evaluation are tabulated in appendices A 3 and A 4. The complicated results of the scalar integrations were contracted with the Landau gauge vector propagators using a symbolic manipulation program. The result can be most simply expressed when all three graphs are combined:

$$\delta\lambda_{\text{eff}}^{(1,m,n)} = f^{abc} f^{abc} g^6 \int_{pq} \mathcal{F}_{pqr} h_2(p, q, r), \quad (5.12)$$

where

$$\begin{aligned} h_2(p, q, r) = & -(p+q-r)(p-q+r)(-p+q+r) \\ & \times \left[\frac{2\mu^2}{(p+q+r)^3} + \frac{\mu(p+q+r+2\mu)}{4pqr} \right. \\ & \left. + \frac{(p+q+r+2\mu)^2}{32p^2q^2r^2(p+q+r)} (p^4+q^4+r^4+6p^2q^2+6p^2r^2+6q^2r^2) \right] \end{aligned} \quad (5.13)$$

and

$$\mu \equiv aNg^2. \quad (5.14)$$

Our prescription for dealing with divergences replaces

$$\begin{aligned} \delta\lambda_{\text{eff}}^{(1,m,n)} & \rightarrow f^{abc} f^{abc} g^6 \int_{pq} [\mathcal{F}_{pqr} h_2(p, q, r) + 3f_p^3 q^{-2} \sin^2 \theta_{pq}] \\ & = f^{abc} f^{abc} g^6 \mu^{-2} \kappa_2, \end{aligned} \quad (5.15)$$

where

$$\begin{aligned} \kappa_2 & = \frac{1}{8\pi^4} \int_0^\infty dp dq \int_{-1}^1 d(\cos \theta) [p^2 q^2 \mathcal{F}_{pqr} h_2(p, q, r) + 3p^2 f_p^3 \sin^2 \theta]_{\mu=1} \\ & = -0.01573(1) \end{aligned} \quad (5.16)$$

and the value of κ_2 has been obtained by direct numerical integration.¹¹

¹¹ The integral can be reduced to a two-dimensional integral by the rewriting $p_{<} = xp_{>}$ and integrating analytically over p , giving something too ugly to reproduce here.

Putting everything together, the final result for the tricritical value of λ/g^2 is

$$\begin{aligned}\lambda/g^2 &= \frac{36}{\pi^2} \left[N^{-1} - \left(\frac{512}{3} \pi^2 \kappa_2 - \frac{4096}{9\pi^2} \kappa_1 - 1 + \frac{128}{3\pi^2} \right) N^{-2} + O(N^{-3}) \right] \\ &= \frac{36}{\pi^2} \left[N^{-1} + 20.8 N^{-2} + O(N^{-3}) \right].\end{aligned}\tag{5.17}$$

We thank Larry Yaffe, Lowell Brown, David Boulware, and Krishna Rajagopal for useful conversations. This work was supported by the U.S. Department of Energy, grant DE-FG03-96ER40956.

APPENDIX A: USEFUL INTEGRALS

1. Scalar integrals

$$z_{ij} \equiv |\mathbf{p}_i - \mathbf{p}_j| \quad (\text{A1})$$

$$\int_l \frac{1}{(\mathbf{l} - \mathbf{p}_1)^2 (\mathbf{l} - \mathbf{p}_2)^2} = \frac{1}{8z_{12}} \quad (\text{A2})$$

$$\int_l \frac{1}{(\mathbf{l} - \mathbf{p}_1)^2 (\mathbf{l} - \mathbf{p}_2)^2 (\mathbf{l} - \mathbf{p}_3)^2} = \frac{1}{8z_{12}z_{23}z_{31}} \quad (\text{A3})$$

$$\int_l \frac{1}{l^2 (\mathbf{l} - \mathbf{p}_1)^2 (\mathbf{l} - \mathbf{p}_2)^2 (\mathbf{l} - \mathbf{p}_1 - \mathbf{p}_2)^2} = \frac{1}{8p_1 p_2 \mathbf{p}_1 \cdot \mathbf{p}_2} \left(\frac{1}{|\mathbf{p}_1 - \mathbf{p}_2|} - \frac{1}{|\mathbf{p}_1 + \mathbf{p}_2|} \right) \quad (\text{A4})$$

Using dimensional regularization for the infrared:

$$\int_l \frac{1}{l^4} = 0 \quad (\text{A5})$$

$$\int_l \frac{1}{l^4 (\mathbf{l} - \mathbf{p})^2} = 0 \quad (\text{A6})$$

$$\int_l \frac{1}{l^4 (\mathbf{l} - \mathbf{p}_1)^2 (\mathbf{l} - \mathbf{p}_2)^2} = \frac{\mathbf{p}_1 \cdot \mathbf{p}_2}{8p_1^3 p_2^3 |\mathbf{p}_1 - \mathbf{p}_2|} \quad (\text{A7})$$

There is a very simple way to evaluate the triangle integral (A3). First shift $\mathbf{l} \rightarrow \mathbf{l} + \mathbf{p}_3$.

Then simply change variables again by a conformal inversion:

$$\mathbf{l} \rightarrow \frac{\mathbf{l}}{l^2}, \quad (\text{A8})$$

and rewrite $\mathbf{p}_1 - \mathbf{p}_3$ and $\mathbf{p}_2 - \mathbf{p}_3$ in terms of

$$\mathbf{q}_1 = \frac{\mathbf{p}_1 - \mathbf{p}_3}{(\mathbf{p}_1 - \mathbf{p}_3)^2}, \quad \mathbf{q}_2 = \frac{\mathbf{p}_2 - \mathbf{p}_3}{(\mathbf{p}_2 - \mathbf{p}_3)^2}. \quad (\text{A9})$$

The result is proportional to the bubble integral (A2), which is trivial to evaluate.

The same technique can be used for the integral (A7), which is easiest to implement by instead considering the convergent integral

$$\int_l \left[\frac{1}{l^4 (\mathbf{l} - \mathbf{p}_1)^2 (\mathbf{l} - \mathbf{p}_2)^2} - \frac{1}{l^4 p_1^2 p_2^2} \right]. \quad (\text{A10})$$

The inversion relates this to an integral of the form

$$\int_l \left[\frac{l^2}{(1 - \mathbf{p}_1)^2 (1 - \mathbf{p}_2)^2} - \frac{1}{l^2} \right] = \frac{\mathbf{p}_1 \cdot \mathbf{p}_2}{8z_{12}}, \quad (\text{A11})$$

which is easy to evaluate.

The integral (A4) can be reduced to the others by rewriting the numerator in terms of denominators as

$$1 = \frac{1}{2\mathbf{p}_1 \cdot \mathbf{p}_2} \left[l^2 + (1 - \mathbf{p}_1 - \mathbf{p}_2)^2 - (1 - \mathbf{p}_1)^2 - (1 - \mathbf{p}_2)^2 \right]. \quad (\text{A12})$$

It is the only specific case we need of the more general result

$$\begin{aligned} & \int_l \frac{1}{(1 - \mathbf{p}_1)^2 (1 - \mathbf{p}_2)^2 (1 - \mathbf{p}_3)^2 (1 - \mathbf{p}_4)^2} = \\ & \frac{1}{8(z_{12}z_{34} + z_{13}z_{24} + z_{14}z_{23})} \left[\frac{1}{z_{12}z_{13}z_{14}} + \frac{1}{z_{21}z_{23}z_{24}} + \frac{1}{z_{31}z_{32}z_{34}} + \frac{1}{z_{41}z_{42}z_{43}} \right]. \end{aligned} \quad (\text{A13})$$

2. Angular averages

$$\left\langle \frac{1}{|\mathbf{p} + \mathbf{q}|} \right\rangle_\theta = \frac{1}{p_>} \quad (\text{A14})$$

$$\left\langle \frac{\cos \theta}{|\mathbf{p} + \mathbf{q}|} \right\rangle_\theta = -\frac{p_<}{3p_>^2}, \quad (\text{A15})$$

$$\left\langle \frac{1}{\cos \theta} \left(\frac{1}{|\mathbf{p} - \mathbf{q}|} - \frac{1}{|\mathbf{p} + \mathbf{q}|} \right) \right\rangle_\theta = \frac{2}{\sqrt{p^2 + q^2}} \text{Sinh}^{-1} \frac{p_<}{p_>} \quad (\text{A16})$$

3. Feynman parameter integrals needed for SU(2) scalar loops

$$\mathcal{F}_\alpha[f(x, y, z)] \equiv \int_0^1 dx dy dz \frac{f(x, y, z) \delta(1 - x - y - z)}{(yzw_1^2 + zxw_2^2 + xyw_3^2)^\alpha} \quad (\text{A17})$$

The w_i are positive scalars.

$$\mathcal{F}_{3/2}[1] = \frac{2\pi}{w_1 w_2 w_3} \quad (\text{A18})$$

$$\mathcal{F}_{3/2}[x] = \frac{2\pi}{w_2 w_3 (w_1 + w_2 + w_3)} \quad (\text{A19})$$

$$\mathcal{F}_{3/2}[x^2] = \frac{\pi}{w_2 w_3} \left[\frac{1}{(w_1 + w_2 + w_3)} + \frac{w_1}{(w_1 + w_2 + w_3)^2} \right] \quad (\text{A20})$$

$$\mathcal{F}_{3/2}[xy] = \frac{\pi}{w_3(w_1 + w_2 + w_3)^2} \quad (\text{A21})$$

$$\mathcal{F}_{3/2}[x^3] = \frac{\pi}{4w_2w_3} \left[\frac{3}{(w_1 + w_2 + w_3)} + \frac{3w_1}{(w_1 + w_2 + w_3)^2} + \frac{2w_1^2}{(w_1 + w_2 + w_3)^3} \right] \quad (\text{A22})$$

$$\mathcal{F}_{3/2}[x^2y] = \frac{\pi}{4w_3} \left[\frac{1}{(w_1 + w_2 + w_3)^2} + \frac{2w_1}{(w_1 + w_2 + w_3)^3} \right] \quad (\text{A23})$$

$$\mathcal{F}_{3/2}[xyz] = \frac{\pi}{2(w_1 + w_2 + w_3)^3} \quad (\text{A24})$$

$$\mathcal{F}_{1/2}[1] = \frac{\pi}{w_1 + w_2 + w_3} \quad (\text{A25})$$

$$\mathcal{F}_{1/2}[x] = \frac{\pi}{4} \left[\frac{1}{(w_1 + w_2 + w_3)} + \frac{w_1}{(w_1 + w_2 + w_3)^2} \right] \quad (\text{A26})$$

The $\mathcal{F}_{3/2}$ results can be obtained from the $\mathcal{F}_{1/2}$ results by differentiating with respect to the w_i and using $x + y + z = 1$.

4. Scalar integrals needed for SU(2)

$$\mathbf{J} \equiv z_{12}\mathbf{p}_3 + z_{23}\mathbf{p}_1 + z_{31}\mathbf{p}_2 \quad (\text{A27})$$

$$\mathbf{K} \equiv \mathbf{p}_1 + \mathbf{p}_2 + \mathbf{p}_3 \quad (\text{A28})$$

$$\int_l \frac{l_i}{(1 - \mathbf{p}_1)^2(1 - \mathbf{p}_2)^2(1 - \mathbf{p}_3)^2} = \frac{J_i}{8z_{12}z_{23}z_{31}(z_{12} + z_{23} + z_{31})} \quad (\text{A29})$$

$$\begin{aligned} \int_l \frac{l_i l_j}{(1 - \mathbf{p}_1)^2(1 - \mathbf{p}_2)^2(1 - \mathbf{p}_3)^2} &= \frac{\delta_{ij}}{16(z_{12} + z_{23} + z_{31})} + \frac{J_i J_j}{16z_{12}z_{23}z_{31}(z_{12} + z_{23} + z_{31})^2} \\ &\quad + \frac{z_{12}p_{3i}p_{3j} + z_{23}p_{1i}p_{1j} + z_{31}p_{2i}p_{2j}}{16z_{12}z_{23}z_{31}(z_{12} + z_{23} + z_{31})} \end{aligned} \quad (\text{A30})$$

$$\begin{aligned} \int_l \frac{l_i l_j l_k}{(1 - \mathbf{p}_1)^2(1 - \mathbf{p}_2)^2(1 - \mathbf{p}_3)^2} &= -\frac{J_i \delta_{jk} + J_j \delta_{ki} + J_k \delta_{ij}}{64(z_{12} + z_{23} + z_{31})^2} - \frac{K_i \delta_{jk} + K_j \delta_{ki} + K_k \delta_{ij}}{64(z_{12} + z_{23} + z_{31})} \\ &\quad - \frac{J_i J_j J_k}{32z_{12}z_{23}z_{31}(z_{12} + z_{23} + z_{31})^3} - \frac{\langle 9z_{12}^2 p_{3i} p_{3j} p_{3k} + 18z_{12} z_{13} p_{2i} p_{2j} p_{3k} \rangle}{64z_{12}z_{23}z_{31}(z_{12} + z_{23} + z_{31})^2} \\ &\quad - \frac{\langle 9z_{12} p_{3i} p_{3j} p_{3k} \rangle}{64z_{12}z_{23}z_{31}(z_{12} + z_{23} + z_{31})} \end{aligned} \quad (\text{A31})$$

The angle brackets in the last expression denote averaging over all permutations of (i, j, k) and all permutations of $(\mathbf{p}_1, \mathbf{p}_2, \mathbf{p}_3)$.

APPENDIX B: SUMMARY OF DIAGRAMS

1. U(1) case: Feynman gauge

$$\begin{aligned}
\delta\lambda_{\text{eff}}^{(\text{a,c,h,r})} &= \text{eq. (3.13c)} \\
&= Ng^8 \int_{pq} \left[3f_p f_q^3 + (3 - 2C_\lambda)^2 f_p^2 f_q^2 + 3f_p^3 f_q \right] \left(-\frac{6}{\pi^2 \Lambda} \right) \\
&= Ng^8 \int_{pq} \mathcal{F}_{pq} \left(-\frac{6}{\pi^2 \Lambda} \right) + Ng^8 \int_{pq} f_p^3 f_q \left(-\frac{24}{\pi^2 \Lambda} \right)
\end{aligned} \tag{B1}$$

$$\begin{aligned}
\delta\lambda_{\text{eff}}^{(\text{b,g,q})} &= \text{eq. (3.13b)} \\
&= Ng^8 \int_{pq} \left[f_p f_q^3 + (3 - 2C_\lambda) f_p^2 f_q^2 + 3f_p^3 f_q \right] \left(\frac{6}{q} + \frac{12}{\pi^2 \Lambda} \right) \\
&= Ng^8 \int_{pq} \mathcal{F}_{pq} \left[\frac{1}{p_{>}} (3 + 3x^{-1}) + \frac{12}{\pi^2 \Lambda} \right] + Ng^8 \int_{pq} f_p^3 f_q \left(\frac{12}{q} + \frac{24}{\pi^2 \Lambda} \right)
\end{aligned} \tag{B2}$$

$$\begin{aligned}
\delta\lambda_{\text{eff}}^{(\text{f})} &= \text{eq. (3.13a)} \\
&= Ng^8 \int_{pq} \mathcal{F}_{pq} \left[-\frac{6}{p} - \frac{6}{q} - \frac{6}{|\mathbf{p} + \mathbf{q}|} + \frac{3 \cos \theta}{2|\mathbf{p} + \mathbf{q}|} + \frac{3(p^2 + q^2)}{pq|\mathbf{p} + \mathbf{q}|} - \frac{6}{\pi^2 \Lambda} \right] \\
&= Ng^8 \int_{pq} \mathcal{F}_{pq} \left[\frac{1}{p_{>}} \left(-12 - 3x^{-1} + \frac{5}{2}x \right) - \frac{6}{\pi^2 \Lambda} \right]
\end{aligned} \tag{B3}$$

$$\begin{aligned}
\delta\lambda_{\text{eff}}^{(\text{i})} &= \text{eq. (3.1)} \\
&= Ng^8 \int_{pq} \mathcal{F}_{pq} \frac{1}{p_{>}} (-9)
\end{aligned} \tag{B4}$$

$$\begin{aligned}
\delta\lambda_{\text{eff}}^{(\text{j})} &= \text{eqs. (3.5, 3.7)} \\
&= Ng^8 \int_{pq} \mathcal{F}_{pq} \frac{1}{p_{>}} (18 - 4x)
\end{aligned} \tag{B5}$$

$$\begin{aligned}
\delta\lambda_{\text{eff}}^{(\text{k})} &= -6Ng^8 \int_{pq} \mathcal{F}_{pq} \int_l \frac{(2\mathbf{l} - \mathbf{p}) \cdot (2\mathbf{l} - \mathbf{p} + 2\mathbf{q})(2\mathbf{l} + \mathbf{q}) \cdot (2\mathbf{l} - 2\mathbf{p} + \mathbf{q})}{l^2(1 - \mathbf{p})^2(1 + \mathbf{q})^2(1 - \mathbf{p} + \mathbf{q})^2} \\
&= Ng^8 \int_{pq} \mathcal{F}_{pq} \int_l \left[-\frac{6}{p} - \frac{6}{q} + \frac{9(p^2 + q^2)}{2pq} \left(\frac{1}{|\mathbf{p} + \mathbf{q}|} + \frac{1}{|\mathbf{p} - \mathbf{q}|} \right) \right. \\
&\quad \left. + \left(\frac{3(2p^4 + 5p^2q^2 + 2q^4)}{4pq\mathbf{p} \cdot \mathbf{q}} - \frac{3\mathbf{p} \cdot \mathbf{q}}{pq} \right) \left(\frac{1}{|\mathbf{p} + \mathbf{q}|} - \frac{1}{|\mathbf{p} - \mathbf{q}|} \right) \right] \\
&= Ng^8 \int_{pq} \mathcal{F}_{pq} \frac{1}{p_{>}} \left[-6 + 3x^{-1} + 7x \right. \\
&\quad \left. - \left(\frac{15}{2} + 3x^{-2} + 3x^2 \right) (1 + x^2)^{-1/2} \text{Sinh}^{-1}x \right]
\end{aligned} \tag{B6}$$

The graphs of figs. 4d and e and the second term in the mass counter-term 3.12 have been ignored above, as they trivially cancel each other.

The infrared divergences of (B1) through (B3) were regulated with dimensional regularization, but, for the sake of making cancelations explicit, we have put the linear divergences back in by hand by writing

$$\int_l \frac{1}{l^4} = \frac{1}{2\pi^2\Lambda}, \quad (\text{B7})$$

where Λ is an infrared momentum cut-off.

2. Abelian graphs: Landau gauge

$$s(x) \equiv \begin{cases} 1, & \text{U(1) theory} \\ x, & \text{SU(2) theory} \end{cases} \quad (\text{B8})$$

$$\delta\lambda_{\text{eff}}^{(\text{a-d,g,h,q,r})} = s\left(\frac{9}{128}\right) Ng^8 \int_{pq} f_p^3 f_q \frac{12}{q} \quad (\text{B9})$$

$$\delta\lambda_{\text{eff}}^{(\text{f})} = s\left(\frac{9}{128}\right) Ng^8 \int_{pq} \mathcal{F}_{pq} \frac{1}{p_{>}} \left(-8 + 4x - \frac{4}{5}x^2\right) \quad (\text{B10})$$

$$\delta\lambda_{\text{eff}}^{(\text{i})} = s\left(\frac{3}{128}\right) Ng^8 \int_{pq} \mathcal{F}_{pq} \frac{1}{p_{>}} \left(-4 - \frac{2}{5}x^2\right) \quad (\text{B11})$$

$$\delta\lambda_{\text{eff}}^{(\text{j})} = s\left(\frac{3}{128}\right) Ng^8 \int_{pq} \mathcal{F}_{pq} \frac{1}{p_{>}} \left(8 - 4x + \frac{4}{5}x^2\right) \quad (\text{B12})$$

$$\delta\lambda_{\text{eff}}^{(\text{k})} = s\left(-\frac{3}{128}\right) Ng^8 \int_{pq} \mathcal{F}_{pq} \frac{1}{p_{>}} \left[-2 + 3x^{-1} + \frac{11}{2}x + \frac{2}{5}x^2 \right. \\ \left. - \left(\frac{15}{2} + 3x^{-2} + 3x^2\right) (1+x^2)^{-1/2} \text{Sinh}^{-1}x \right] \quad (\text{B13})$$

For non-Abelian graphs, see eqs. (5.6), (5.8) and (5.12).

REFERENCES

- [1] D. Kirzhnits and A. Linde, Phys. Lett. **D9**, 2257 (1974); Ann. Phys. **101**, 195 (1976).
- [2] J. Chen, T. Lubensky, and D. Nelson, Phys. Rev. **B17**, 4274 (1978).
- [3] P. Arnold and L. Yaffe, Phys. Rev. **D49**, 3003 (1994); Univ. of Washington preprint UW/PT-96-28 (errata).
- [4] K. Kajantie, M. Laine, K. Rummukainen, and M. Shaposhnikov, Phys. Rev. Lett. **77**, 2887 (1996).
- [5] I. Kondor and T. Temesvari, J. Physique Lett. (Paris) **39**, L99, L415(E) (1978); Y. Okabe and M. Oku, Prog. Theor. Phys. **60**, 1277, 1287 (1978); **61**, 443 (1979).
- [6] G. Baker, D. Meiron, and B. Nickel, Phys. Rev. Lett. **58**, 1365 (1978); *Compilation of 2-pt. and 4-pt. graphs for continuous spin models*, University of Guelph report (1977), unpublished.
- [7] F. Wilczek, Int. J. Mod. Phys. **A7**, 3911 (1992).
- [8] K. Kanaya and S. Kaya, Phys. Rev. **D51**, 2404 (1995).
- [9] B. Halperin, T. Lubensky, and S. Ma, Phys. Rev. Lett. **32**, 292 (1974).
- [10] A. Aharony, Phys. Rev. B **8**, 4270 (1973); P. Arnold and L. Yaffe, Univ. of Washington report UW/PT-96-23.
- [11] G. 't Hooft, in *Recent developments in gauge theories*, ed. G. 't Hooft *et al.* (Plenum, 1980).
- [12] S. Elitzur, Phys. Rev. **D12**, 3978 (1975).
- [13] E. Braaten and A. Nieto, Phys. Rev. **D51**, 6990 (1995); K. Farakos, K. Kajantie, M. Shaposhnikov, Nucl. Phys. **B425**, 67 (1994); P. Arnold in “Proceedings of the Eighth International Seminar Quarks ‘94: Vladimir, Russia,” ed. D. Yu. Grigoriev, *et.al.* (World

Scientific: Singapore, 1995).

- [14] E. Fradkin and S. Shenkar, Phys. Rev. **D19**, 3682 (1979); S. Elitzur, Phys. Rev. **D12**, 3978 (1975).